Design of a Wideband Omnidirectional Antenna With Characteristic Mode Analysis

Xu Yang, Ying Liu, *Senior Member, IEEE*, and Shu-Xi Gong, *Member, IEEE*

***Abstract*—A low-profile horizontally polarized (HP) omnidirectional metasurface-inspired antenna is presented. To realize HP omnidirectional radiation pattern, the theory of characteristic mode is utilized to facilitate the analysis of three antenna structures. Then, by properly exciting the desired characteristic mode, the antenna with a wide bandwidth and good omnidirectionality, which is based on the modification of the standard patch antenna, is obtained. The simulated results show that the proposed antenna not only can obtain a low profile of $0.06\lambda_0$ (where λ_0 is the free-space wavelength at 5.2 GHz), but also has a wide operating bandwidth of 16.6%. Finally, the metasurface-inspired antenna is manufactured and the error analysis between the simulated and measured results is also provided. The antenna can be applied to 5G wireless local area network systems.**

***Index Terms*—5G wireless local area network (WLAN), characteristic mode analysis (CMA), low-profile, metasurface-inspired, omnidirectional, wideband.**

I. Introduction

HORIZONTALLY polarized (HP) omnidirectional antenna can radiate electromagnetic waves with 360° coverage in the horizontal plane and has a certain beamwidth in the vertical plane. Hence, it has many applications in indoor and urban areas, such as the wireless local area network (WLAN) systems and radio frequency identification system.

During the past decades, a number of designs have been proposed to realize omnidirectional antennas. It is well known that Alford loop antennas [1], [2] are studied to achieve HP omnidirectional patterns. However, the limited bandwidth restricts their applications. Dipole antenna and monopole antenna can also be used to obtain HP omnidirectional radiation patterns. In [3], a circularly polarized omnidirectional antenna composed of four bended monopoles was excited by the cross-power distribution network. Although this antenna had a compact size, the problem of a narrow bandwidth still could not be solved, and the bended structures would make manufacturing more difficult. An array with an improved feeding network, which consisted of a modification of the original planar dipoles and parasitic dipoles, was proposed in [4]. The antenna could realize omnidirectional radiation patterns over a wide frequency band, but it had a complicated structure and a large longitudinal size.

Meanwhile, in order to design a more compact omnidirectional antenna, some antennas based on metamaterials [5]–[9] have been investigated. For instance, a mu-negative transmission-line loop antenna array [9] was proposed to yield an HP omnidirectional radiation pattern over a wide frequency band, but the large antenna size was needed and the bandwidth of an element achieved was relatively narrow. Thus, to simultaneously address the problem of compact size and wide operating band of the metamaterial antenna, one kind of metasurface antenna has drawn much attention [10]–[13]. Especially in [13], by choosing the proper characteristic mode with characteristic mode analysis (CMA) [14]–[16], the metasurface was effectively excited to achieve a wide operating bandwidth.

In this letter, to achieve HP omnidirectional radiation patterns and a low profile over a wide frequency band, three antenna structures are studied with the theory of characteristic mode (TCM) within the 5 GHz band. The CMA is an effective analytical method that can offer physical insight of the radiation mechanism of an antenna. With its help, the better feeding positions can be found [17]. The contribution of this work is that to realize the omnidirectional radiation pattern, by means of CMA, a standard patch structure is optimized. Then, the antenna comprising 4×4 square patches is simultaneously excited by four slots with an equal amplitude and phase to realize the desired radiation pattern over a wide frequency band. Also, simulated results indicate that the proposed antenna obtains wide operating bandwidths and relatively small antenna size. Then, in order to verify the performances of the antenna, the proposed antenna is manufactured and tested.

II. Mechanism of the Metasurface-Inspired Antenna

A. Analysis of the Characteristic Mode

Three antenna structures without the feeding parts are shown in Fig. 1. They are denoted as types I–III, respectively. Type I is a traditional microstrip square patch. As for types II and III, both structures are based on the modifications of type I. Then, in order to investigate the radiation characteristics, TCM is utilized to analyze the structures by using commercial simulation software CST 2016. The substrate with a relative dielectric constant of 4.4 and loss tangent of 0.02 is employed.

Fig. 2 depicts the modal significances (MSs), indicating the coupling capability of each characteristic mode with the external sources [18]. It can be seen that several MSs are greater than

Manuscript received March 20, 2018; accepted April 17, 2018. Date of publication April 20, 2018; date of current version June 4, 2018. This work was supported by the National Natural Science Foundation of China under Grant 61372001. *(Corresponding author: Ying Liu.)*

The authors are with the National Key Laboratory of Antennas and Microwave Technology, Collaborative Innovation Center of Information Sensing and Understanding, Xidian University, Xi'an 710071, China (e-mail: liuying@mail.xidian.edu.cn).

Digital Object Identifier 10.1109/LAWP.2018.2828883

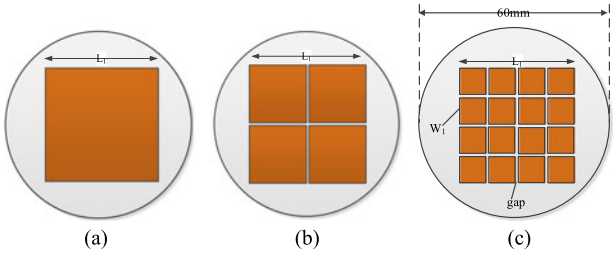

Fig. 1. Configuration of three antennas without feeding parts. (a) Type I. (b) Type II. (c) Type III.

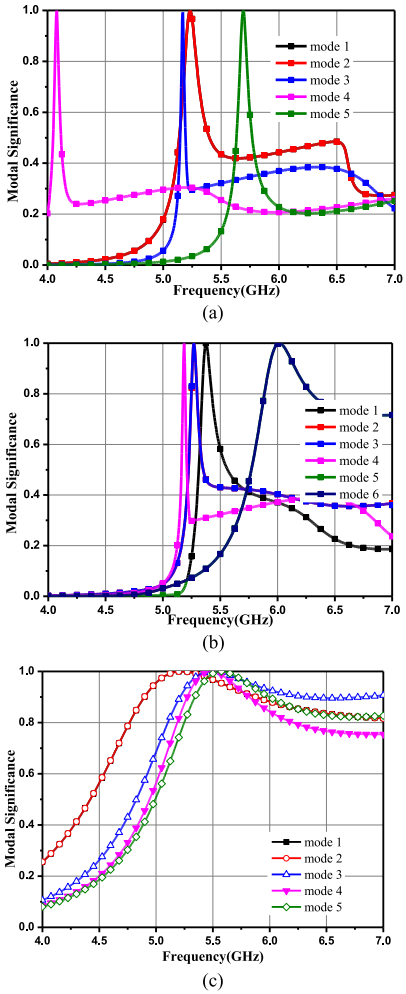

Fig. 2. MSs of the three structures. (a) Type I. (b) Type II. (c) Type III.

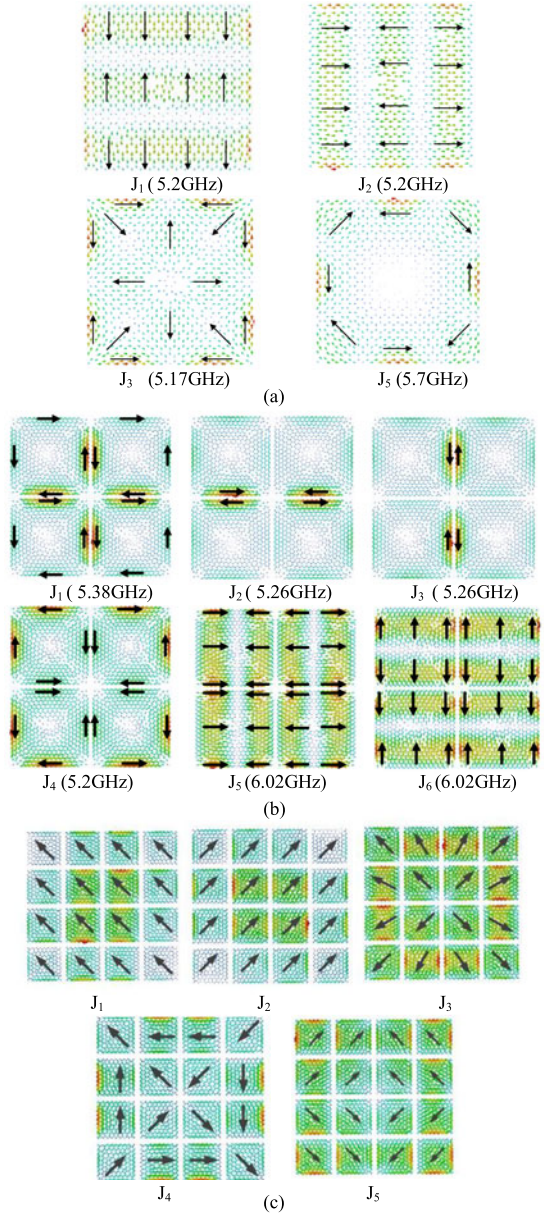

Fig. 3. Modal currents corresponding to the MSs of the three structures. (a) Modal currents of type I. (b) Modal currents of type II. (c) Modal currents of type III at 5.5 GHz.

0.7 from 5 to 6 GHz, which means that theses modes may be excited effectively. For types I and II, the modes have narrow resonant frequency band, compared with the modes of type III. Also, some modes (modes 1 and 2 of type I, modes 2 and 3 of type II, modes 5 and 6 of type II, and modes 1 and 2 of type III) have the same MSs. However, the MS does not account for the radiation characteristics. Then, the modal current is analyzed.

The modal currents of the three structures are illustrated in Fig. 3. J_n represents the modal surface current of mode n. Because of the narrow resonant band for types I and II, the modal currents, which are at the resonant frequencies, respectively, are shown in Fig. 3(a) and (b). Unfortunately, none of the modes can be excited to realize the desired radiation pattern for types I and II within the desired band. However, it should be noted from Fig. 4(a) that the modal radiation pattern of mode 1, for type II, is close to the omnidirectional radiation pattern. Here, mode 4 of type I is not discussed because the mode is not desired and the resonant frequency is lower than 5 GHz band. For Type III, it can be observed from Fig. 3(c) that the surface current J_3 of type II is very similar to that of a monopolar patch antenna, which means the mode may be excited effectively to realize an omnidirectional radiation pattern. Thus, the modal radiation pattern is simulated in Fig. 4(b). A good omnidirectional radiation pattern is obtained.

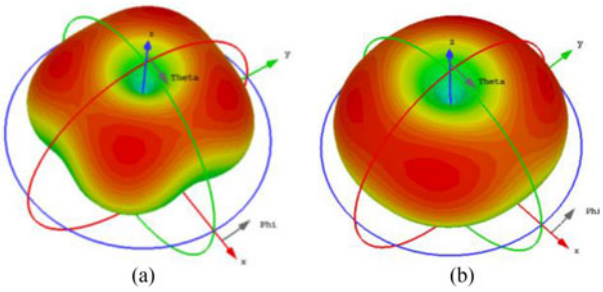

Fig. 4. Modal radiation patterns of types II and III at the resonant frequencies. (a) Mode 1 (5.38 GHz). (b) Mode 3 (5.5 GHz).

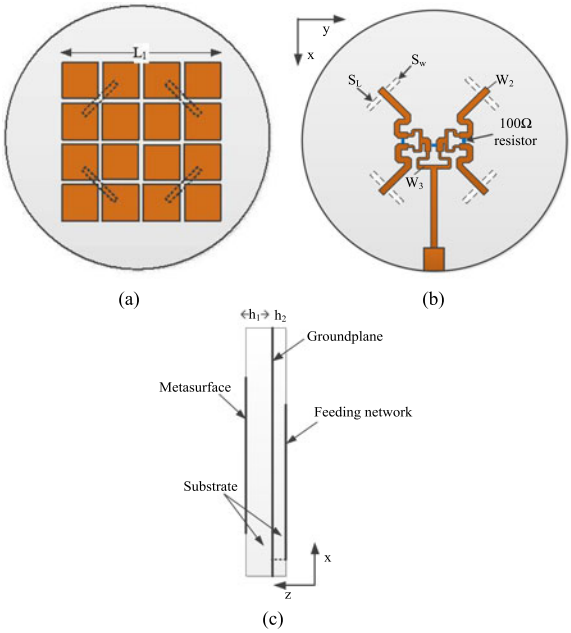

Fig. 5. Structure of the proposed antenna. (a) Top view. (b) Feeding network. (c) Side view.

B. Wideband Omnidirectional Metasurface-Inspired Antenna

Based on the analysis above, the modal current J_3 of type III is investigated in detail. It is easy to find that the maximum current distribution located at the four corners of the metasurface is where the characteristic mode can be excited effectively. The method of aperture coupling feed is adopted. Four symmetrical slots etched on the ground plane are placed right under the four corners of the slotted patch. Furthermore, to keep amplitudes and phases of the four ports equal, a one-to-four Wilkinson power divider is utilized. Fig. 5 shows the configuration of the proposed antenna. The optimized geometric parameters of the antenna are listed in Table I.

It can be observed from Fig. 6 that the antenna obtains a –10 dB impedance bandwidth of 16.6%. Furthermore, to verify that the desired mode has been excited properly, a surface current distribution of the antenna at 5.5 GHz is shown in Fig. 7. The currents on the metasurface flow in the opposite direction, causing a deep null in the broadside direction of the radiation pattern of the vertical plane. In other words, the radiation pattern of the antenna resembles that of a monopolar patch antenna.

TABLE I
PARAMETERS OF THE PROPOSED ANTENNA (UNIT: mm)

Parameters	Value
L_1	38.2
W_1	8.8
W_3	0.73
S_L	16
S_W	1.6
h_1	3
h_2	0.8
gap	1

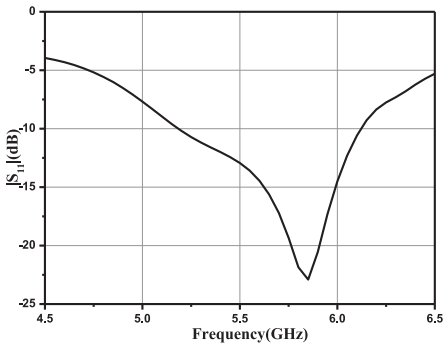

Fig. 6. Simulated S_{11} of the proposed antenna.

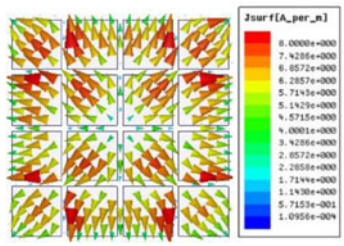

Fig. 7. Simulated surface current distribution at 5.5 GHz of the proposed antenna.

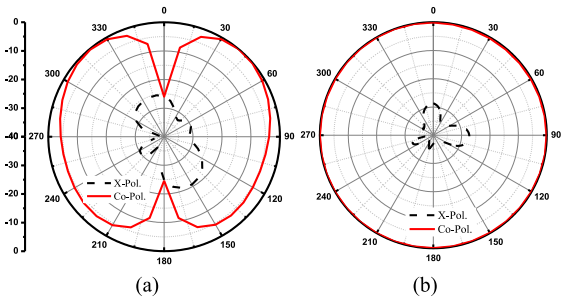

Fig. 8. Simulated radiation patterns of the proposed antenna at 5.8 GHz. (a) Radiation pattern in the vertical plane ($\phi = 0^o$). (b) Radiation pattern in the horizontal plane ($\theta = 40^o$).

Also, contrasting the simulated surface current of the antenna and modal current J_3 of type III, the mode 3 is excited well.

Fig. 8 shows the radiation patterns of the proposed antenna in the vertical plane ($\phi = 0^o$) and the horizontal plane ($\theta = 40^o$) where the maximum realized gain exists at 5.8 GHz. It can be known that the gain variation in the horizontal plane is less than 3 dB over the wide frequency band. Also, a low profile of $0.06\lambda_0$ is obtained.

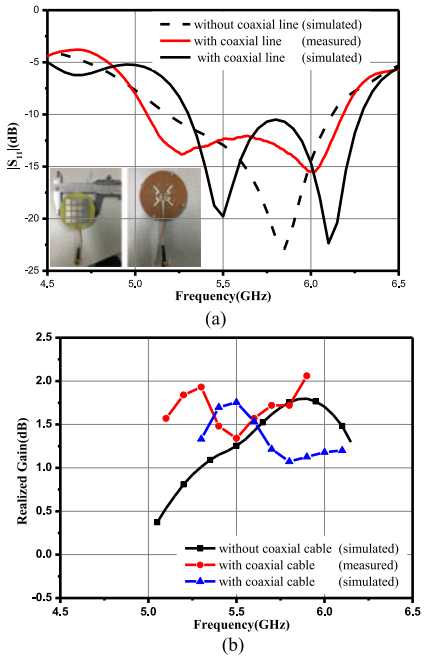

Fig. 9. Measured (a) S_{11} and (b) realized gain of the antenna.

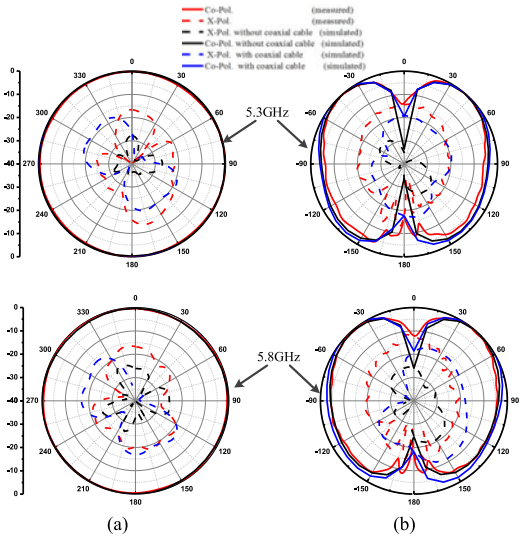

Fig. 10. Measured and simulated normalized radiation patterns of the proposed antenna. (a) Radiation patterns in the horizontal plane ($\theta = 40^{o}$). (b) Radiation patterns in the vertical plane ($\phi = 0^{o}$).

III. Experimental Results of the Proposed Antenna

To validate the simulated results of the proposed metasurface-inspired antenna, the antenna is fabricated and measured. Also, the fabricated antenna is measured using the vector network analyzer Agilent N5230C, and the radiation characteristics are measured in the Satimo SG 128 spherical near-field chamber.

Fig. 9(a) shows the measured S_{11} of the proposed antenna. The operating frequency band of the manufactured antenna spans from 5.06 to 6.18 GHz. The fractional bandwidth is 19.9%. Fig. 9(b) plots the measured realized gain of the antenna. However, it can be seen that there exist some differences between the measured and simulated results. The main reason is caused by the unbalance of the coaxial cable. Moreover, the antenna with the coaxial cable is simulated, and the results can be found in Figs. 9 and 10. In addition, manufactured tolerance and measurement errors may lead to the differences too.

Fig. 10 plots the measured and simulated normalized radiation patterns of the antenna. The coaxial cable also makes the cross polarization deteriorate, which can be seen from the figure. Table II shows the comparison of antenna size, operating bandwidth, etc., in the open literature. It can be clearly observed that the proposed antenna has a wider operating bandwidth than the previous antennas.

TABLE II
Comparison of the Performances Among Previous Works and the Proposed Antenna

Ref.	Dimension (λ_0)	Bandwidth (%)	Gain (dB)	polarization
5	Diameter>2	4.38	~4.9	Linear polarization
7	Diameter=1.15	5.6	~5.6	Linear polarization
proposed	Diameter=1.13	16.6	0.5-1.8	Linear polarization

IV. Conclusion

A low-profile HP omnidirectional metasurface-inspired antenna was designed. The theory of the characteristic mode was utilized to facilitate the analysis procedure for three antenna structures. Then, a slotted patch antenna based on the modification of the standard patch antenna was chosen to be excited effectively by the four symmetrical slots, so that a good omnidirectional radiation characteristic was obtained. The proposed antenna not only had a low profile of $0.06\lambda_0$, but also achieved a wide operating bandwidth of 16.6%. The proposed antenna can be a good candidate for WLAN applications.

References

[1] A. Alford and A. G. Kandoian, "Ultrahigh-frequency loopantennas," *Elect. Eng.*, vol. 59, no. 12, pp. 843–848, Dec. 1940.
[2] C. H. Ahn, S. W. Oh, and K. Chang, "A dual-frequency omnidirectional antenna for polarization diversity of MIMO and wireless communication applications," *IEEE Antennas Wireless Propag. Lett.*, vol. 8, pp. 966–969, 2009.
[3] Y. Yu, Z. Shen, and S. He, "Compact omnidirectional antenna of circular polarization," *IEEE Antennas Wireless Propag. Lett.*, vol. 11, pp. 1466–1469, 2012.
[4] Y. Yu, J. Xiong, and R. Wang, "A wideband omnidirectional antenna array with low gain variation," *IEEE Antennas Wireless Propag. Lett.*, vol. 15, pp. 386–389, 2016.
[5] A. Al-Zoubi, F. Yang, and A. Kishk, "A low-profile dual-band surface wave antenna with a monopole-like pattern," *IEEE Trans. Antennas Propag.*, vol. 55, no. 12, pp. 3404–3412, Dec. 2007.
[6] S. Chaimool, T. Pechrkool, P. Akkaraekthalin, and K. Chung, "A compact zeroth-order resonant antenna based on modified Jerusalem mushroom structures," in *Proc. Int. Workshop Antenna Technol.*, Sydney, NSW, Australia, 2014, pp. 348–350.
[7] F. Yang, Y. Rahmat-Sami, and A. Kishk, "Low-profile patch-fed surface wave antenna with a monopole-like radiation pattern," *Microw., Antennas Propag.*, vol. 1, no. 1, pp. 261–266, Feb. 2007.
[8] B. C. Park *et al.*, "Omnidirectional circularly polarized antenna using zeroth-order resonance of metamaterial transmission line," in *Proc. 4th Eur. Conf. Antennas Propag.*, Barcelona, Spain, 2010, pp. 1–2.

[9] K. Wei, Z. Zhang, Z. Feng, and M. F. Iskander, "A MNG-TL loop antenna array with horizontally polarized omnidirectional patterns," *IEEE Trans. Antennas Propag.*, vol. 60, no. 6, pp. 2702–2710, Jun. 2012.

[10] W. Liu, Z. N. Chen, and X. Qing, "Metamaterial-based low-profile broadband aperture-coupled grid-slotted patch antenna," *IEEE Trans. Antennas Propag.*, vol. 63, no. 7, pp. 3325–3329, Jul. 2015.

[11] M. Martinis, L. Bernard, K. Mahdjoubi, R. Sauleau, and S. Collardey, "Wideband antenna in cavity based on metasurfaces," *IEEE Antennas Wireless Propag. Lett.*, vol. 15, pp. 1053–1056, 2016.

[12] Z. Wu, L. Li, Y. Li, and X. Chen, "Metasurface superstrate antenna with wideband circular polarization for satellite communication application," *IEEE Antennas Wireless Propag. Lett.*, vol. 15, pp. 374–377, 2016.

[13] F. H. Lin and Z. N. Chen, "Low-profile wideband metasurface antennas using characteristic mode analysis," *IEEE Trans. Antennas Propag.*, vol. 65, no. 4, pp. 1706–1713, Apr. 2017.

[14] R. J. Garbacz and R. H. Turpin, "A generalized expansion for radiated and scattered fields," *IEEE Trans. Antennas Propag.*, vol. AP-19, no. 3, pp. 348–358, May 1971.

[15] R. F. Harrington and J. R. Mautz, "Theory of characteristic modes for conducting bodies," *IEEE Trans. Antennas Propag.*, vol. AP-19, no. 5, pp. 622–628, Sep. 1971.

[16] R. F. Harrington and J. R. Mautz, "Computation of characteristic modes for conducting bodies," *IEEE Trans. Antennas Propag.*, vol. AP-19, no. 5, pp. 629–639, Sep. 1971.

[17] Y. Chen and C. F. Wang, "Characteristic-mode-based improvement of circularly polarized U-slot and E-shaped patch antennas," *IEEE Antennas Wireless Propag. Lett.*, vol. 11, pp. 1474–1477, 2012.

[18] Y. Chen and C. F. Wang, *Characteristic Modes: Theory and Applications in Antenna Engineering*. New York, NY, USA: Wiley, 2015.